

# Picosecond time resolved photoluminescence spectroscopy of a tetracene film on highly oriented pyrolytic graphite: Dynamical relaxation, trap emission, and superradiance

M. Voigt and A. Langner

*Institut für Physikalische und Theoretische Chemie der Universität Bonn, Wegelerstrasse 12, 53115 Bonn, Germany*

P. Schouwink

*Max-Planck-Institut für Polymerforschung, Mainz, Germany*

J. M. Lupton

*Max-Planck-Institut für Polymerforschung, Mainz, Germany and Department of Physics, University of Utah, 115 South 1400 East, Salt Lake City, Utah 84112-0830*

R. F. Mahrt

*Max-Planck-Institut für Polymerforschung, Mainz, Germany and IBM Research Laboratory, Rüschlikon CH-8803, Switzerland*

M. Sokolowski<sup>a)</sup>

*Institut für Physikalische und Theoretische Chemie der Universität Bonn, Wegelerstrasse 12, 53115 Bonn, Germany*

(Received 13 April 2007; accepted 3 July 2007; published online 19 September 2007)

A detailed time resolved investigation of the photoluminescence of a thin tetracene film deposited on highly oriented pyrolytic graphite is presented. In agreement with Lim *et al.* [Phys. Rev. Lett. **92**, 107402 (2004)], we find strong evidence for superradiance: an increase of the relative intensity of the pure electronic transition with respect to the vibronic sideband and a concomitant decrease of the radiative lifetime from 10 to 1.83 ns upon cooling from 300 to 4 K. For lower temperatures, a redshift ( $\sim 200 \text{ cm}^{-1}$ ) of the free exciton is observed. Previously, this shift was attributed to a structural phase transition. Our time resolved spectra reveal that the spectral shift is related to a dynamical relaxation process which occurs within the first 50 ps. © 2007 American Institute of Physics. [DOI: 10.1063/1.2766944]

## I. INTRODUCTION

Tetracene (Tc, see inset of Fig. 1) is a model molecule that has been used for investigations of fundamental photo-physical processes of  $\pi$ -conjugated materials in the condensed phase for many years.<sup>1,2</sup> Recent interesting experiments concerning the optical properties of Tc are, e.g., the realization of light emitting organic field effect transistors based on Tc films<sup>3</sup> and the observation of a superradiant light emission from Tc nanoaggregates and films.<sup>4</sup> The interpretation of the photoluminescence (PL) spectra of Tc crystals<sup>1,2</sup> and films<sup>4-6</sup> is, however, not as straightforward as may be expected for this small molecule. Phase transitions as a function of temperature<sup>7</sup> can modify the luminescence properties, and fluorescence from different trap states also appears to play a pronounced role in the emission properties. As a consequence, significant variations of the PL spectra were found dependent of sample history and preparation<sup>1</sup> for bulk crystals and, in particular, for films.<sup>5</sup> In addition, the PL emission lines have a considerable width ( $\sim 1000 \text{ cm}^{-1}$ ), even at low temperatures and for pure and structurally perfect crystals,<sup>1</sup> which makes the spectral interpretation more difficult. In this

aspect Tc differs significantly from, e.g., quaterthiophene (4T), which has a comparable molecular size but yields sharp PL lines [full width at half maximum (FWHM) of  $\sim 50 \text{ cm}^{-1}$ ].<sup>8</sup>

Time resolved PL measurements should give more detailed information on the emission processes in structural aggregates of Tc. Time resolved PL spectra of Tc *films* as a function of temperature were measured early on by Peter and Bässler<sup>9</sup> in the nanosecond time range and later with an improved time resolution by Wappelt *et al.*<sup>10</sup> Several relaxation processes with time constants in the range of 260 ps to 1.2 ns were identified,<sup>10</sup> leading to nonexponential decays. However, as we will demonstrate, these processes do *not* reflect the *intrinsic* excitonic properties which occur on a shorter time scale of about 100 ps.

Time resolved PL data for Tc films in the subnanosecond range were recently reported by Lim *et al.*<sup>4</sup> At room temperature (RT), the authors found a biexponential decay with a time constant  $\tau_{\text{PL}}$  of the shorter-lived component of 82 ps. Lim *et al.* also measured the fluorescence yield  $\Phi$  and calculated a radiative lifetime  $\tau_{\text{rad}}$  of the Tc film at RT of 12.5 ns ( $\tau_{\text{rad}} = \Phi^{-1} \tau_{\text{PL}}$ ). Since this value is smaller by about a factor of 2 than  $\tau_{\text{rad}}$  of isolated Tc molecules in solution,<sup>11,12</sup> Lim *et al.* concluded that the fluorescence in Tc films occurs

<sup>a)</sup> Author to whom correspondence should be addressed. Fax: +49-(0)228-73 2551. Electronic mail: sokolowski@pc.uni-bonn.de

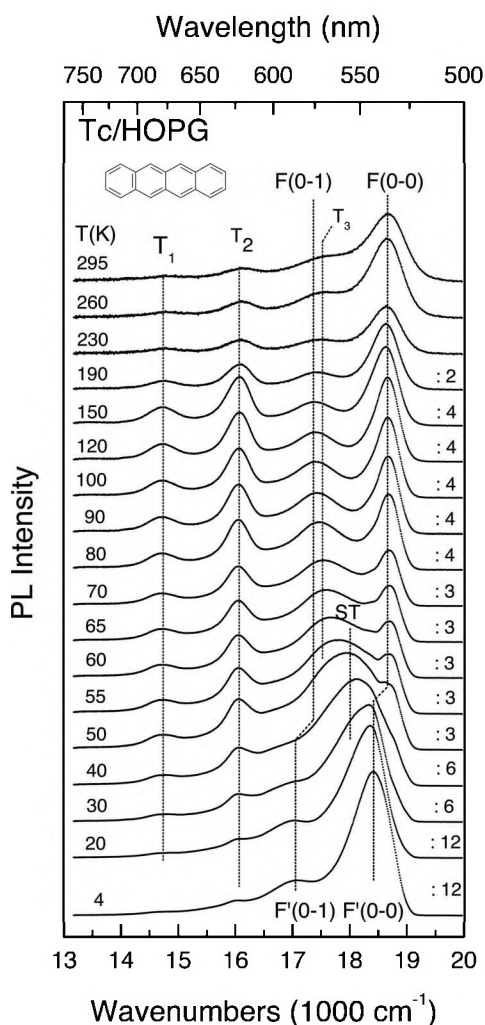


FIG. 1. Time-integrated photoluminescence spectra of a polycrystalline film of tetracene (Tc) on highly oriented pyrolytic graphite (HOPG) recorded at different temperatures. The spectra are shifted vertically against each other for clarity.  $F(0-0)$ ,  $F(0-1)$ , and  $F'(0-0)$ ,  $F'(0-1)$  mark positions of the 0-0 and the 0-1 transitions of two types of free excitons. ST marks the transition of a self-trapped exciton, and  $T_1$ ,  $T_2$ , and  $T_3$  mark luminescent traps. The respective vertical lines at these positions are lines to guide the eye. The intensities at low temperatures were scaled; the corresponding numbers are given on the right hand side. The inset shows the structure formula of tetracene. For further details, see text.

via a *superradiant* decay mechanism. Additional support for this superradiant decay process via a short-lived *coherent exciton state* was based on the observed weakening of the first vibronic sideband (0-1 transition) at lower temperatures.<sup>4</sup> This superradiance of Tc aggregates is a consequence of the herringbone arrangement of the transition dipoles in the *ab* plane of the Tc crystal lattice and has been investigated theoretically in detail by Spano.<sup>13-16</sup>

In the present paper we report an extended investigation of the time resolved PL spectra of Tc films in the picosecond time domain, where the temperature was varied to provide an additional parameter influencing the sample morphology and the exciton dynamics. As we will demonstrate, the understanding of the spectra requires consideration of several photophysical processes, namely, the presence of at least two different emitting states and several luminescent trap states.

In addition, we show that the radiative lifetime  $\tau_{\text{rad}}$  decreases by over an order of magnitude for small temperatures. This finding is in agreement with what is expected for a superradiant decay in Tc aggregates, which was suggested by Lim *et al.*<sup>4</sup> This lifetime shortening is a consequence of the higher coherence of the exciton states at low temperatures due to smaller phonon scattering. We expand on the results of Lim *et al.* by considering both emission relating to trapping states as well as to two distinct structural phases of the Tc film. Our results are important for understanding and optimizing device performance in organic electronics. Excitonic delocalization in superradiance may ultimately be of importance to designing electrically driven organic lasers, provided a suitable feedback geometry can be attained under the condition of high excitation densities.

## II. EXPERIMENT

The Tc was purchased from Aldrich and purified by two cycles of gradient sublimation. The Tc film was prepared by vacuum deposition under a base pressure of  $3 \times 10^{-6}$  mbar and a deposition rate of 1 nm/min on freshly cleaved highly oriented pyrolytic graphite (HOPG). The films are expected to be polycrystalline with the *ab* plane parallel to the substrate, leading to a nearly perpendicular orientation of the long molecular axis with respect to the substrate plane.<sup>17</sup> A small nominal film thickness of only  $\sim 7$  nm was chosen in order to keep effects due to structural defects resulting from coalescence of Tc crystallites to a minimum.<sup>18</sup>

The PL experiments were carried out in the time resolved mode and for comparison also in the time-integrated mode. Cooling was achieved in a static flow He cryostat with the sample kept at different temperatures between 4 and 300 K. For optical excitation, frequency doubled pulses with 80 MHz repetition rate from a Ti-sapphire laser were used. The wavelength was 430 nm, and the temporal pulse width was less than 150 fs. For the time-integrated PL measurements, an excitation power of 150  $\mu\text{W}$  (spot diameter of 50–100  $\mu\text{m}$ ) was used; for the time resolved measurements, the time-averaged excitation power was 200  $\mu\text{W}$ . We note that no spectral changes were observed in time-integrated spectra upon variation of the excitation power. For time-integrated detection, a 0.3 m monochromator (Acton Research Corporation) in combination with a Hamamatsu charge coupled device (CCD) camera (S 7031-1007) was employed. The spectral resolution was about 0.5 nm ( $20 \text{ cm}^{-1}$ ). Time resolved detection was performed with a 0.25 m monochromator in combination with a synchroscan streak camera (C5680) and a CCD camera (C 4742-95), both from Hamamatsu. As a consequence, the nominal spectral resolution of the time resolved spectra was smaller than for the cw spectra, which explains the slightly narrower 0-0 lines of the cw spectra compared to the time resolved PL spectra in Fig. 2. The time resolution was 6 ps, as determined from the rising edge of decay curves (see below). The maximal time window covered in time resolved measurements was 2 ns. From the two-dimensional data sets, taken as a function of wave numbers and delay time, time resolved spectra and decay curves<sup>19</sup> were extracted (see Figs. 3 and 4). The time

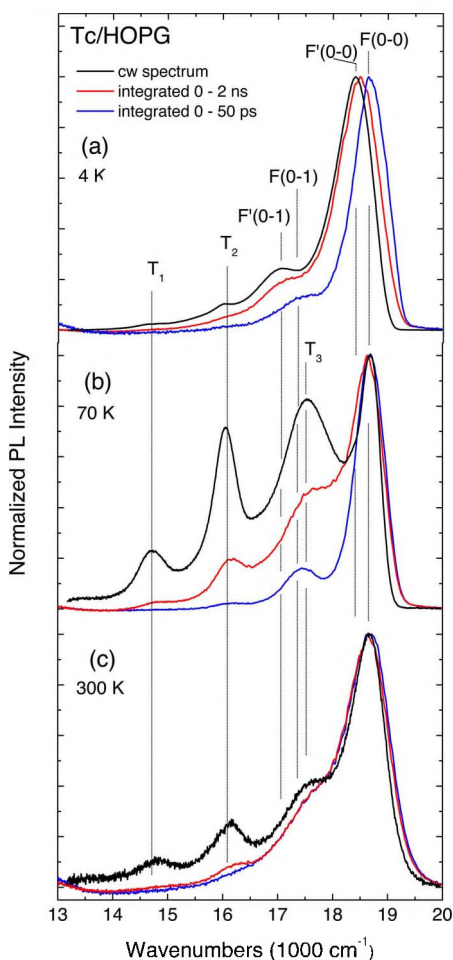


FIG. 2. (Color online) Photoluminescence spectra of a tetracene film on HOPG at three different temperatures (a) 4 K, (b) 70 K, and (c) 300 K. Blue lines: spectra integrated over the first 50 ps; red lines: spectra integrated over the first 2 ns, and black lines: cw spectra. All spectra were normalized to maximum intensity. The lettering and the marked positions are identical to those of Fig. 1.

interval for the time resolved spectra was 10 ps. In addition, spectra were extracted which were integrated over delay time for the first 50 ps or the first 2 ns (see Fig. 2).

Time-integrated PL spectra were taken upon cooling and warming up of the sample. The time resolved spectra were measured during the warm-up only. Cooling from room temperature took about 1 h, whereas the warm-up took about 2 h.

### III. RESULTS AND INTERPRETATION

#### A. Time-integrated photoluminescence spectra

We start with an overview on the time-integrated (cw) PL spectra as a function of temperature, which are shown in Fig. 1. The main emission line is found at  $18600\text{ cm}^{-1}$  at 295 K. Upon cooling, it shifts by  $\sim 200\text{ cm}^{-1}$  to smaller energies at temperatures of about 50 K. In PL spectra of single crystals, these two line positions were assigned to 0-0 transitions of two types of *free excitons* (termed as the *F* and *F'* state).<sup>1,2,20</sup> Accordingly, they are labeled as *F*(0-0) and *F'*(0-0) in the following. For Tc single crystals, the *F*→*F'* shift was observed at slightly higher temperatures of

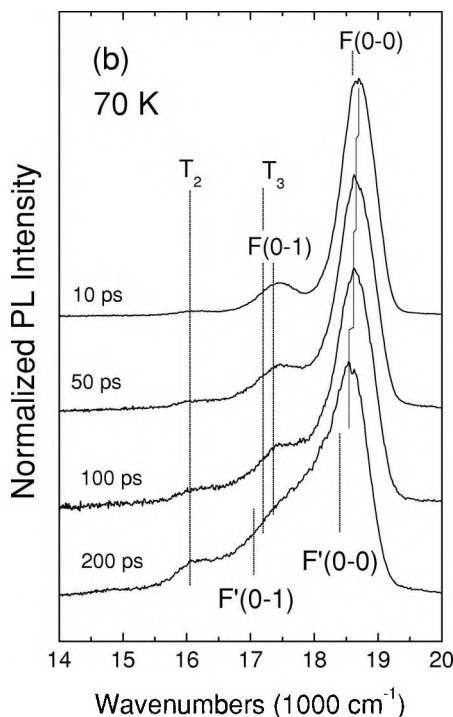
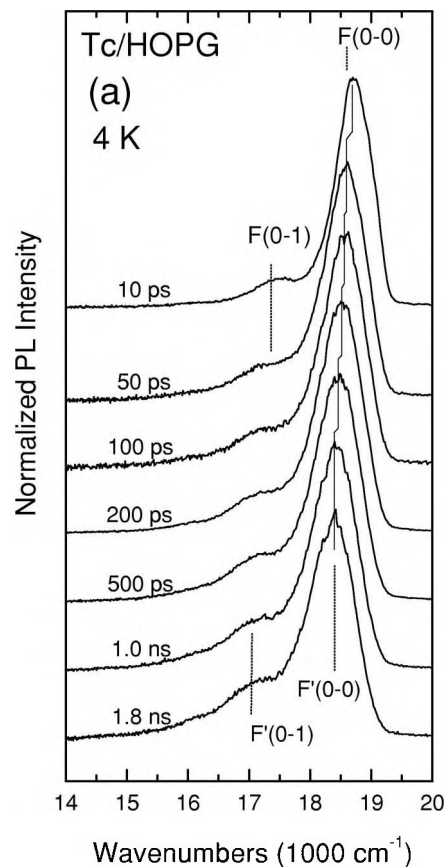


FIG. 3. Time resolved photoluminescence spectra of a tetracene film on HOPG for different delay times: (a) at 4 K and (b) at 70 K. All spectra were normalized to maximum intensity. The spectra are shifted vertically against each other for clarity. The labeling and the marked spectral features are identical to those of Fig. 1. The positions of the maxima are marked by vertical lines in order to demonstrate the shift of the maxima with time.

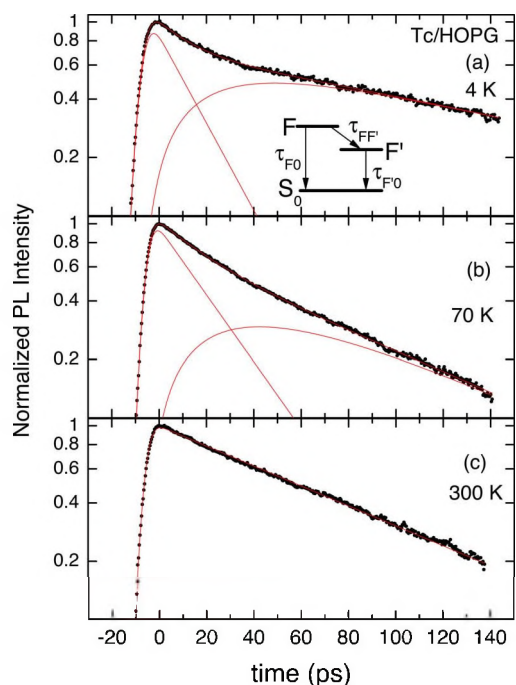


FIG. 4. (Color online) Decay curves of the integrated fluorescence intensity of a tetracene film on HOPG for three different temperatures: (a) 4 K, (b) 70 K, and (c) 300 K. A time independent background was subtracted, and the curves were normalized to maximum intensity. The scaling factors with respect to the curve at 300 K are 6.80 and 3.88 for the curves at 4 K and 70 K, respectively. The solid line (red) is a fit to the data according to Eq. (1) which describes the emission via two consecutive emissive states  $F$  and  $F'$ . The intensity contributions of these two states are also plotted separately. The experimental resolution is described by a convolution with a Gaussian instrument response function with a FWHM of 6 ps. The inset in (a) illustrates the decay scheme. For further details, see text.

60–100 K.<sup>1,2</sup> This line shift was also found for polycrystalline Tc films prepared on other substrates.<sup>6</sup>

A likely origin for the  $F \rightarrow F'$  shift is a structural phase transition which is observed for Tc crystals between 80 and 130 K.<sup>7</sup> The phase transition leads to a second, also triclinic, phase at low temperatures with slightly different lattice parameters and an approximately 5% smaller volume of the unit cell.<sup>7,23,24</sup> This phase transition is, however, not well reproducible and a wide range of transition temperatures has been reported in the literature (see Refs. 1 and 7 and discussions therein). This scatter of the transition temperatures is likely due to finite size and hysteresis effects. Finite size effects may be also the reason why the transition occurs at slightly lower temperatures in our spectra (50 K instead of 80–130 K). In addition, there exists the possibility that the structural packing of Tc in our thin films differs slightly with respect to that of the bulk crystal structure, causing the noted difference. Thin film phases have been reported extensively for the homologue molecule pentacene<sup>25</sup> and lately also for Tc.<sup>22</sup>

In the following we will denote the two corresponding Tc phases as the *high* and *low* temperature (HT and LT) phases of Tc. We note, however, that simultaneous measurements of structural and PL spectra have not been performed yet, and the assignment of  $F$  and  $F'$  to the two structural phases is hence indirect. In addition, it turns out from our

time resolved data that a static picture is *not* sufficient, but different dynamic evolutions after excitation occur in the two phases, i.e., excitation energy can be transferred from the  $F$  to the  $F'$  state but also to trap states. However, for our initial description we simply assign the two emitting states as  $F$  and  $F'$  to the two different structural phases of Tc.

Both the  $F(0-0)$  and the  $F'(0-0)$  line exhibit only one very weak vibronic sideband. These are marked by  $F(0-1)$  and  $F'(0-1)$  in Fig. 1. We note that these sidebands are composed of several unresolved vibronic modes, as can be seen from highly resolved spectra of Tc dissolved in liquid He droplets<sup>26</sup> or glass.<sup>27</sup> The sidebands are significantly weaker compared to those observed for Tc in solution.<sup>4,12</sup> This difference can be understood by the superradiant character of the emission<sup>4</sup> (see below) and/or a smaller structural distortion of the excited Tc molecule in the solid phase compared to the liquid, leading to a smaller Franck-Condon factor. The energies of the corresponding vibronic modes  $\nu_1$  and  $\nu'_1$  are found to be 1230 and 1420  $\text{cm}^{-1}$ , respectively. We tentatively explain this difference in vibrational energy of the two phases by the different crystal lattices in the HT and LT phases in combination with the nonlocal, phononlike character of the vibration.

In addition to the peaks described so far, three distinct luminescent trap states (marked by  $T_1$ ,  $T_2$ , and  $T_3$ ) at 14 730, 16 050, and 17 520  $\text{cm}^{-1}$  can be identified in Fig. 1. Emission from these trap states is weak at the extremities of the investigated temperature range, i.e., at 295 and 4 K, and strongest at temperatures from about 80 to 150 K. Likely structural defects, possibly due to an incomplete structural phase transition, play a role in the radiative emission of excitons at trap states. This interpretation is supported by the strong changes of the relative intensity of the trap luminescence (up to a factor of about 10), which are observed for different warming and cooling cycles of the sample across the phase transition. Finally, a clear indication that these spectral features result from trap states and are hence *not* intrinsic luminescence properties coming from the time resolved spectra in Figs. 2(a)–2(c): in the spectra integrated over the first 50 ps, the lines  $T_1$ ,  $T_2$ , and  $T_3$  are absent (at all temperatures); in the spectra integrated over the first 2 ns, they have *only small* intensities compared to the cw spectra. This shows that these states are filled by slower relaxation processes, i.e., exciton migration to traps. For other polycrystalline films,<sup>6,28</sup> emission from  $T_1$ ,  $T_2$ , and  $T_3$  were observed with different intensities, presumably due to variations in the structural quality, thus supporting the above assignment of the transition lines to traps.

In addition to  $T_1$ ,  $T_2$ , and  $T_3$ , a broad line marked by ST (18 000  $\text{cm}^{-1}$ ) is seen in a small temperature range around 55 K, i.e., the temperature range in which the phase transition occurs. This feature is assigned to a *self-trapped* (ST) exciton in the literature,<sup>1</sup> and is hence also a nonintrinsic luminescence line. Its appearance may also be related to the instability of the Tc lattice in the region of the phase transition.<sup>1</sup>

## B. Time resolved spectra and decay curves

In the following we will concentrate on the *intrinsic* emission features, which are particularly prominent in the first 50 to 100 ps. These short time spectra are contrasted to the cw spectra in Fig. 2 as well as spectra recorded in an integration window of 2 ns. Figure 3 shows spectra which were drawn from the time resolved data set for specific delay times, illustrating the complete spectral evolution with time. Decay curves which show the wavelength integrated intensities versus time are displayed in Fig. 4.

### 1. 300 K spectra

We start with the discussion of the data at 300 K. As seen in Fig. 2(c), the spectra integrated in time over the first 50 ps and the first 2 ns are very similar. This indicates the presence of *one* luminescent species. The decay curve of the integrated intensity is shown in Fig. 4(c). It can be well fitted by a monoexponential decay which is convoluted by a Gaussian with a FWHM of 6 ps in order to describe the instrument response function. Hence, at room temperature, we find a simple first-order decay process of one emitting species. The corresponding time constant  $\tau_F^{300\text{ K}}$  is determined as  $84 \pm 5$  ps, and is in very good agreement with the value of 82 ps reported by Lim *et al.*<sup>4</sup>

The filling of the trap states  $T_1$ ,  $T_2$ , and  $T_3$  at delay times above 2 ns was already mentioned above. For an integration time of up to 2 ns these contribute only very little to the spectrum [see Fig. 2(c)].

### 2. 4 K spectra

At 4 K a surprising evolution of the spectra with time is observed. This evolution occurs mainly within the first 100 ps and can be seen clearly in the series of spectra which covers the first 1.8 ns displayed in Fig. 3(a). The 10 ps spectrum corresponds to the emission spectrum of the  $F$  state. With time, the spectrum gradually shifts to lower energies, and at about 200 ps the spectrum corresponds to that of the  $F'$  species. This coincidence can be seen from the comparison with the corresponding line positions of the 0-0 and the 0-1 transitions of the  $F$  and  $F'$  states, which were taken from the cw spectra and which are indicated in Fig. 3(a). In this case, the largest shift of the 0-0 line position already occurs within the first 50 ps.

Thus, for short times we identify the  $F$  state as the emitting state, as it is observed at high temperatures. Remarkably, in the cw spectra taken at 4 K, this  $F$  emission is *not* visible at all. At times above  $\sim 200$  ps the emission occurs solely from the  $F'$  state [see Fig. 3(a)], and only this emission determines the cw spectra. This latter finding can in particular be seen in Fig. 2(a), which demonstrates that the 2 ns integrated spectra and the cw spectrum (both predominantly from the  $F'$  state) are nearly identical, whereas the 50 ps spectrum is shifted to higher wave numbers by  $200\text{ cm}^{-1}$  (corresponding to the  $F$  state).

The emission from two different species ( $F$  and  $F'$ ) is also reflected by the decay curve at 4 K [see Fig. 4(a)]. It shows a fast decay for roughly the first 40 ps, which corresponds to the emission from the  $F$  state, and then crosses

over to a slower, approximately exponential decay, which corresponds to emission from the  $F'$  state. The simplest kinetic model which describes these observations is equivalent to that of two consecutive first-order reactions<sup>29</sup> and can be parameterized as the following: the state  $F$  decays with a time constant  $\tau_F$  ( $1/\tau_F = 1/\tau_{F0} + 1/\tau_{FF'}$ ) which includes the radiative or nonradiative decay into the ground state ( $S_0$ ) with a time constant  $\tau_{F0}$  and a feeding of the state  $F'$  with a time constant  $\tau_{FF'}$ . The state  $F'$  in turn decays via a time constant  $\tau_{F'0}$  into the ground state or trap states. A schematic illustration of the model is given in the inset of Fig. 4. This model yields the following time dependence for the intensity:<sup>29</sup>

$$I(t) = A_F \exp(-t/\tau_F) + A_{F'} [\exp(-t/\tau_{F'0}) - \exp(-t/\tau_{FF'})]. \quad (1)$$

The first term describes the luminescent decay from the  $F$  state, the second that of the  $F'$  state. As shown in Fig. 4(a), the integrated intensity as a function of time can be well fitted by Eq. (1), which indicates the validity of the model. Again, we have used a convolution by a Gaussian to describe the experimental broadening. The amplitudes  $A_F$  and  $A_{F'}$  were taken as free fitting parameters. In Fig. 4(a), the contributions of the luminescent decays of the  $F$  and  $F'$  state are also separately indicated. As described above, the luminescence from the state  $F$  decays within the first 40 ps, while the luminescence of  $F'$  builds up due to feeding from  $F$ , and subsequently decays with a slower time constant. The superposition of the two components with varying prefactors leads to the shift of the 0-0 line within the first 100 ps that was described above [see Fig. 3(a)]. We note that the time resolved spectra between 0 and 100 ps can be well fitted by a weighted superposition of the spectra taken at 0 ps ( $F$  state emission) and 100 ps ( $F'$  state emission). The so obtained time dependence of the relative amplitudes of the fitted spectral components (not shown here) agrees perfectly with that found from the fit by Eq. (1) to the spectrally integrated intensity and additionally confirms the model. From the fit, we determined:  $\tau_{F0}^{4\text{ K}} = 86 \pm 5$  ps,  $\tau_{FF'}^{4\text{ K}} = 25 \pm 5$  ps, and  $\tau_{F'0}^{4\text{ K}} = 168 \pm 5$  ps. This yields  $\tau_F^{4\text{ K}} = 19 \pm 5$  ps ( $1/\tau_F = 1/\tau_{F0} + 1/\tau_{FF'}$ ). The fluorescence decay time  $\tau_F^{4\text{ K}}$  of the  $F$  state is thus found to be smaller by a factor of 0.2 with respect to the decay time of the  $F$  state at 300 K ( $\tau_F^{300\text{ K}} = 84$  ps).

On the basis of these results we have to reconsider the assignment of the two emitting species  $F$  and  $F'$  to emission from two different structural phases (HT/LT) of Tc. The observation of the  $F$  spectrum at short times implies that some regions (crystallites) in the sample must still be in the Tc HT phase, even at low temperatures of 4 K, whereas other regions, likely the majority, are in the LT phase. This would mean that the structural phase transition is significantly incomplete, as discussed above (see Sec. III A). However, such a mixed phase sample morphology would also yield a superposition of emissions from the  $F$  state *and* the  $F'$  state at very short times, which is not observed here. Instead, a rise of the  $F'$  emission due to feeding from  $F$  is found. Hence, an explanation which simply relates the  $F$  and  $F'$  line positions to emission from two structurally different regions in the Tc

film appears unlikely. A more appropriate explanation is the occurrence of a dynamical process, which allows the exciton state to relax in energy by  $200\text{ cm}^{-1}$  within the first 40 ps. The necessary constraint is that this relaxation process from  $F$  to  $F'$  is only possible in the LT phase, whereas it is blocked in the HT phase, and is thus absent at higher temperatures where only the HT phase is present. In this model, the  $F \rightarrow F'$  spectral shift in the cw spectra would hence be an indirect consequence of the structural phase transition. The mechanism of this relaxation to the  $F'$  state is presently unknown. A self-trapping process involving a small local structural distortion of the Tc molecule could be a plausible explanation,<sup>1</sup> which could also explain why the lifetime  $\tau_{F0}^{4\text{ K}} = 168 \pm 5$  ps is considerably larger than  $\tau_F^{4\text{ K}} = 19 \pm 5$  ps. In addition, a direct excitation of the  $F'$  state apparently does not occur at low temperatures, which is understandable in this model, since this state is dynamically formed. Alternatively, the  $F'$  emission could be due to shallow traps which have formed during the structural phase transition.

### 3. 70 K spectra

We conclude by discussing the spectra at 70 K. At this temperature, the emission from the  $F$  state is stronger. The  $F'$  emission occurs at later times with a smaller amplitude compared to the situation at 4 K. This effect can be seen from the cw spectra in Fig. 1 and the time resolved spectra taken within the first 200 ps shown in Fig. 3(b). Furthermore, Fig. 3(b) shows that the emission from the trap states  $T_2$  and  $T_3$  evolves significantly between 100 and 200 ps. In particular, at 200 ps emission from  $T_3$  entirely masks the vibronic side band.

For short times, i.e., below 100 ps, the trap emission is less relevant, and Eq. (1) yields a good fit to the temporal evolution of the integrated intensity [see Fig. 4(b)]. The fitted time constants are  $\tau_{F0}^{70\text{ K}} = 136 \pm 5$  ps,  $\tau_{FF'}^{70\text{ K}} = 31 \pm 5$  ps, and  $\tau_{F'0}^{70\text{ K}} = 79 \pm 5$  ps. This yields  $\tau_F^{70\text{ K}} = 25 \pm 5$  ps. Hence we find  $\tau_F^{4\text{ K}} (=19\text{ ps}) < \tau_F^{70\text{ K}} (=25\text{ ps}) < \tau_F^{100\text{ K}} (=84\text{ ps})$ , and  $\tau_{F'0}^{4\text{ K}} (=168\text{ ps}) > \tau_{F'0}^{70\text{ K}} (=31\text{ ps})$ .

### C. Superradiance

As noted in the Sec. I, Lim *et al.* concluded that the time resolved luminescence of Tc bears evidence for the occurrence of superradiance in the condensed phase.<sup>4</sup> We can confirm this proposal and note that in the present case of our Tc films on HOPG the superradiant emission becomes even stronger at low temperatures. Before turning to our results, we give a brief summary of superradiance in organic crystals. This phenomenon occurs due to the formation of delocalized exciton wave functions (Bloch states), which extend over a number  $N_c$  of molecules.<sup>13–16</sup> As a consequence the oscillator strength of the 0-0 transition, which is proportional to  $\tau_{\text{rad}}^{-1}$ , increases proportional to  $N_c$ . Since the coherence of the wave function and consequently  $N_c$  increases with decreasing temperature due to a reduction in dynamic disorder and exciton scattering effects, an increase of the superradiant emission visible in the intensity of the 0-0 transition is expected at lower temperatures.<sup>30</sup> For polycrystalline quaterthiophene films, Meinardi *et al.*<sup>31</sup> deduced a superradiant

emission from a significant shortening of the radiative lifetime of the 0-0 transition as the temperature was lowered to 4 K. Notably, the phenomenon does *not* occur in the vibronic side band,<sup>15</sup> and hence the 0-1 emission intensity does not scale with  $N_c$ . As a consequence the *relative* intensity of the vibronic side bands decreases for lower temperatures.

The experimental evidence for a superradiant emission in Tc nanoaggregates and films was obtained by Lim *et al.*<sup>4</sup> from a comparison of the fluorescence of isolated Tc molecules in solution and in aggregates. Lim *et al.* found the following for the aggregates with respect to the isolated molecules in solution at room temperature: (i) a greater intensity of the 0-0 transition ( $I_{0-0}$ ) relative to that of the 0-1 vibronic side band ( $I_{0-1}$ ), and (ii) a shortening of the radiative lifetime  $\tau_{\text{rad}} = \tau_F / \Phi$  ( $\Phi$  being the fluorescence quantum yield). In addition, a relative increase of the 0-0 transition with respect to the 0-1 vibronic sideband was also observed for decreasing temperature,<sup>4</sup> which is consistent with the increase of  $N_c$  at low  $T$ , as described above. Nevertheless, the noted redistribution of vibronic intensity should be considered with some caution, since the change of the lattice with temperature and a concomitant change of the electronic interactions between the molecules may induce changes in the Franck-Condon factors, which could also, at least partially, modify the  $I_{0-0}/I_{0-1}$  ratio.

Evidently, our data are in agreement with the findings (i) and (ii) of Lim *et al.* In addition, our data also support the expected relative increase of the 0-0 transition intensity for lower temperatures. From a comparison of the 10 ps spectra in Figs. 3(a) and 3(b), we find the relative intensity of the vibronic sideband  $F(0-1)$  with respect to the  $F(0-0)$  transition to decrease by about 10% as the temperature is lowered from 70 to 4 K. At 300 K, the intensity of the  $F(0-1)$  replica is difficult to determine since it is strongly washed out. However, we estimate it to be twice as strong as at 70 K, which supports the trend described. Interestingly, at 4 K the intensity of the  $F'(0-1)$  vibronic sideband is twice as great as the  $F(0-1)$  vibronic sideband (see Fig. 2(a)), which might indicate that the superradiant emission is more strongly suppressed for the emission from the  $F'$  state.

In addition to confirming the findings of Lim *et al.*,<sup>4</sup> we are able to estimate the shortening of  $\tau_{\text{rad}}^F$  with the decrease in temperature from our data. We calculate  $\tau_{\text{rad}}^F = \tau_F / \Phi$ , where  $\Phi$  is the absolute fluorescence quantum yield for emission from the state  $F$  as a function of temperature. The  $\Phi$  values are proportional to the number of photons emitted from the  $F$  state normalized to the laser excitation power. We determined these from the absolute areas under the exponential decay curves of the  $F$  state in Fig. 4. We note that the  $\Phi$  values *cannot* be read from the relative areas under the cw PL spectra, since these also contain the contributions to the emission from the  $F'$  state, the ST exciton, and the trap states. These contributions would otherwise lead to a wrong value of  $\tau_{\text{rad}}^F$ . Variations in the excitation power and the integration time of the detection were accounted. Since the Tc film was homogeneous across the sample area, small variations of the laser spot position on the sample due to the temperature variation were not meaningful. Nevertheless, we reckon that the  $\Phi$  values are still subject to errors due to

TABLE I. Overview of the fluorescence time constants  $\tau_F$  ( $1/\tau_F = 1/\tau_{F0} + 1/\tau_{FF}$ ) determined from fits to the decay curves according to Eq. (1), the absolute quantum yields  $\Phi$  of the emission from the  $F$  state of tetracene, the radiative time constants  $\tau_{\text{rad}}^F = \tau_F/\Phi$ , and the nonradiative time constants  $\tau_{\text{nonrad}}^F = \tau_F/(1-\Phi)$ . The value of  $\Phi$  at 300 K was taken from Lim *et al.* (Ref. 4). For further details, see text.

Temperature (K)	$\tau_F$ (ps)	$\Phi$ (%)	$\tau_{\text{rad}}^F$ (ns)	$\tau_{\text{nonrad}}^F$ (ps)
300	84	0.8	10.5	85
70	25	0.8	3.01	25
4	19	1.0	1.83	19

variations in the light collection efficiency, which we can, however, not quantify. Notably, the increase in  $\Phi$  upon cooling is rather small, i.e., by only 20% (see Table I). Quite differently, the area under the cw spectra increases considerably upon cooling, namely, by a factor of about 25 (see Fig. 1). This is, however, mainly due to the strong emission from the  $F'$  state that fully dominates the cw spectra at low temperatures, and not due to the emission from the  $F$  state, which is of interest here.

From our data we can, of course, derive only the relative changes of  $\Phi$ . To obtain absolute numbers, we calibrated our values to the quantum yield at room temperature  $\Phi_{300\text{ K}}$  as determined by Lim *et al.*<sup>4</sup> for Tc nanoaggregates in solution ( $\Phi_{300\text{ K}}=0.8\%$ ). An overview on the computed time constants is given in Table I.

We find a decrease in  $\tau_{\text{rad}}^F$  from 300 K (=100%) to about 29% at 70 K and 17% at 4 K. This corresponds to an increase in the decay rate ( $1/\tau_{\text{rad}}^F$ ) by a factor of about 6. Hence, a considerable shortening of the radiative lifetime is obtained at lower temperatures, in agreement with the expectation for superradiance. For comparison, Meinardi *et al.*<sup>31</sup> found a similar reduction of  $\tau_{\text{rad}}$  to about 15% between 120 and 4 K for 4T films. In addition, we find from our data that the time constant of the nonradiative decay of the  $F$  state [ $\tau_{\text{nonrad}}^F = \tau_F/(1-\Phi)$ ] is also reduced from RT to 4 K by a factor of about 4.

Finally, we comment on the relation of the changes in the time domain and the spectral domain as they would be expected on the basis of a superradiant emission from the  $F$  state at low temperatures. With respect to the RT situation, Lim *et al.* found an about consistent increase of the  $I_{0-0}/I_{0-1}$  ratio and  $1/\tau_{\text{rad}}^F$  by about a factor of 3 ( $\sim N_c$ ) at low  $T$ . Here, we find comparable change of  $I_{0-0}/I_{0-1}$ , but by a factor of about 2 stronger increase of  $1/\tau_{\text{rad}}^F$ . At present, we are not able to fully explain this discrepancy. Possible reasons may be (i) the variation of  $\tau_{\text{nonrad}}^F$  as a function of temperature (see Table I), contrary to the situation found by Lim *et al.* where a constant value of  $\tau_{\text{nonrad}}^F$  was seen, and/or (ii) small changes in the Franck-Condon factors as noted above.

## IV. CONCLUDING DISCUSSION

Our time resolved data provide strong evidence for the shortening of the radiative lifetime  $\tau_{\text{rad}}^F$  at lower temperatures which is expected for a superradiant emission. The obtained values of  $\tau_{\text{rad}}^F$  ( $\sim 1.83$  ns) at 4 K are by at least a factor of 16 shorter than the radiative time constant of the isolated Tc

molecule at room temperature, e.g., in solution, which has previously been reported as 27 ns (Ref. 4) and 30 ns.<sup>11</sup> With respect to the film phase at RT ( $\tau_{\text{rad}}^F=10.5$  ns),  $\tau_{\text{rad}}^F$  is reduced by about a factor of 6 at 4 K. Notably, the determination of  $\tau_{\text{rad}}^F$  at low temperatures is complicated by a two-step kinetics of the exciton decay. The exciton ( $F$ ) decays only partly directly to the ground state under emission of light, but in addition feeds a second emitting state ( $F'$ ). The subsequent decay of  $F'$  occurs with a time constant ( $\tau_{F'0}$ ) which is at least a factor of 3 longer compared to that of  $F$  ( $\tau_F$ ). The mechanism of this relaxation from  $F$  to  $F'$  by about  $\sim 200\text{ cm}^{-1}$  is not entirely understood yet. Evidently the relaxation is very fast, since it occurs within the first 40 ps after the excitation. As described above, the relaxation is related to the presence of the low temperature (LT) phase of Tc, since it is only found at low temperatures and is absent at room temperature. Two explanations can be envisaged. The first is based on excitation energy transfer from small (residual) HT phase domains to LT phase domains of Tc within the film. However, this would *not* explain why the fluorescence from the  $F'$  is not observed from the beginning. Hence, an on-site relaxation of the excitation energy in the LT phase is more plausible. This process occurs only for the LT phase, possibly because the above noted slightly denser packing of the molecules in the LT phase compared to the HT phase is a prerequisite for the process. Alternatively, shallow defects may play a role, as noted above.

We find that emission from radiative trap states is observed in the spectra after about 100 ps. Clearly, this observation demonstrates that the intrinsic luminescence processes can only be observed if the time resolution of the experiments is sufficiently below 100 ps. This is also true for the emission from the second, relaxed energy emissive state ( $F'$ ). Only with a sufficient time resolution as employed in the present investigation is it possible to discern the consecutive emission from this state, which is fed from the  $F$  state with a time constant which ranges between  $\tau_{FF}^4\text{ K}=25\pm 5$  ps at 4 K and  $\tau_{FF}^{70\text{ K}}=31\pm 5$  ps at 70 K.

## V. SUMMARY

From time resolved luminescence spectra taken as a function of temperature we identify a decrease of the radiative lifetime of the excitonic fluorescence for lower temperatures. In detail, we find a reduction from 10 to  $\sim 1.8$  ns for a lowering of the temperature from 300 to 4 K. The observed effect is in agreement with the expectation of a superradiant emission as derived by Lim *et al.*<sup>4</sup> However, in addition, we demonstrate that the luminescence kinetics are complicated by the presence of further emissive species, most notably trap states and a second stable morphology which is manifested at low temperatures. Time constants for the luminescence decay via radiative traps (about 100 ps after the excitation) and a relaxation of the exciton energy by about  $200\text{ cm}^{-1}$  at low temperatures within the first 40 ps are identified. These results are important for developing spectroscopic tools for the optical assessment of morphological phases in materials for organic electronics. In addition, the remarkable exciton delocalization, which leads to a lifetime

shortening of a factor of about 16 with respect to the isolated molecules, implies exceptional oscillator strength which makes these materials interesting for quantum optical applications. Such a molecular level control over the radiative exciton lifetime may also be useful in developing strategies for the design of organic laser diodes.<sup>32</sup>

## ACKNOWLEDGMENTS

This work was supported by the Deutsche Forschungsgemeinschaft (DFG) through the priority program "Organic Field Effect Transistors SSP 1121" and the DFG research unit 557 "Light Confinement and Control with Structural Dielectrics and Metals." We are grateful to A. Volz for experimental support. One of us (M.S.) acknowledges helpful discussions with S. Schrader and F. Spano.

<sup>1</sup>H. Nishimura, T. Yamaoka, A. Matsui, K. Mizuno, and G. J. Sloan, *J. Phys. Soc. Jpn.* **54**, 1627 (1985).

<sup>2</sup>K. Mizuno, A. Matsui, and G. J. Sloan, *Chem. Phys.* **131**, 423 (1989).

<sup>3</sup>A. Hepp, H. Heil, W. Weise, M. Ahles, R. Schmechel, and H. von Seggern, *Phys. Rev. Lett.* **91**, 157406 (2003).

<sup>4</sup>S.-H. Lim, T. G. Bjorklund, F. C. Spano, and C. J. Bardeen, *Phys. Rev. Lett.* **92**, 107402 (2004).

<sup>5</sup>H. Müller and H. Bässler, *Chem. Phys. Lett.* **36**, 312 (1975).

<sup>6</sup>A. Langner, Y. Su, and M. Sokolowski, *Phys. Rev. B* **74**, 045428 (2006).

<sup>7</sup>E. Venuti, R. G. Della Valle, L. Farina, A. Brillante, M. Masino, and A. Girlando, *Phys. Rev. B* **70**, 104106 (2004).

<sup>8</sup>W. Gebauer, A. Langner, M. Schneider, M. Sokolowski, and E. Umbach, *Phys. Rev. B* **69**, 125420 (2004).

<sup>9</sup>G. Peter and H. Bässler, *Chem. Phys.* **49**, 9 (1980).

<sup>10</sup>A. Wappelt, A. Bergmann, A. Napiwotzki, H. J. Eichler, H.-J. Jüpner, A. Kummrow, A. Lau, and S. Woggon, *J. Appl. Phys.* **78**, 5192 (1995).

<sup>11</sup>C. Burgdorff, S. Ehrhardt, and H. G. Lohmansröben, *J. Phys. Chem.* **95**, 4246 (1991).

<sup>12</sup>J. B. Birks, *Photophysics of Aromatic Molecules* (Wiley-Interscience, London 1970), p. 123; P. K. McCarthy and G. J. Blanchard, *J. Phys. Chem.* **99**, 17748 (1995).

<sup>13</sup>F. Spano, *Chem. Phys. Lett.* **24**, 7 (2000).

<sup>14</sup>F. Spano, *J. Chem. Phys.* **116**, 5877 (2002).

<sup>15</sup>F. Spano, *J. Chem. Phys.* **118**, 981 (2003).

<sup>16</sup>F. Spano, *J. Chem. Phys.* **120**, 7643 (2004).

<sup>17</sup>S. Hasegawa, H. Inokuchi, K. Seki, and N. Ueno, *J. Electron Spectrosc. Relat. Phenom.* **78**, 391 (1996).

<sup>18</sup>M. Schneider, M. Brinkmann, M. Muccini, F. Biscarini, C. Taliani, W. Gebauer, M. Sokolowski, and E. Umbach, *Chem. Phys.* **285**, 345 (2002).

<sup>19</sup>We note that the integration was performed on the wavelength axis, without a  $1/\lambda^2$  correction. This correction is not relevant in the present case since it modifies the spectra only marginally.

<sup>20</sup>We note that slightly different values for the exact line position of the  $F$  emission were reported in the literature, ranging over about  $200\text{ cm}^{-1}$ . Compare, e.g., Refs. **1**, **2**, **5**, **6**, and **21**. The reason is not quite clear yet, and may be partially due to shortcomings in calibration. For our data, the reason may also be that a thin film phase of Tc with a slightly different packing is formed (Ref. **22**). For the present data, the time resolved spectra were shifted by  $100\text{ cm}^{-1}$  to higher energies with respect to the cw spectra, ensuring consistency between the two data sets. The small difference in the energy scale is likely due to the use of two different monochromators for the two types of measurements.

<sup>21</sup>S. V. Frolov, Ch. Kloc, J. H. Schön, and B. Batlogg, *Chem. Phys. Lett.* **334**, 65 (2001).

<sup>22</sup>S. Milita, M. Servidori, F. Cicoria, C. Santato, and A. Pifferi, *Nucl. Instrum. Methods Phys. Res. B* **246**, 101 (2006).

<sup>23</sup>U. Sondermann, A. Kutoglu, and H. Bässler, *J. Phys. Chem.* **89**, 1735 (1985).

<sup>24</sup>D. Holmes, S. Kumaraswamy, A. J. Matzger, and K. P. Voilhardt, *Chem.-Eur. J.* **5**, 3399 (1999) and references therein.

<sup>25</sup>C. M. Mattheus, A. B. Dros, J. Baas, G. T. Oostergetel, A. Meetsma, J. L. de Boer, and T. M. Palstra, *Synth. Met.* **138**, 475 (2003).

<sup>26</sup>R. Lehnig and A. Slenczka, *J. Chem. Phys.* **122**, 244317 (2005).

<sup>27</sup>A. Elschner and H. Bässler, *Chem. Phys.* **112**, 285 (1987).

<sup>28</sup>M. Voigt, Diplomarbeit, Universität Bonn 2001.

<sup>29</sup>See, e.g., R. A. Alberty and R. J. Silbey, *Physical Chemistry* (Wiley, New York, 1992).

<sup>30</sup>We note that this type of superradiance of Frenkel excitons is not a cooperative emission and occurs in the limit of low exciton densities too.

<sup>31</sup>F. Meinardi, M. Cerminara, A. Sassella, R. Bonifacio, and R. Turbino, *Phys. Rev. Lett.* **91**, 247401 (2003).

<sup>32</sup>M. A. Baldo, R. J. Holmes, and S. R. Forrest, *Phys. Rev. B* **66**, 035321 (2002).